Accepted Article

Title: Interface between an Au(111) surface and an ionic liquid: The influence of water on the double layer capacitance

Authors: Jochen Friedl; Iulius I.E. Markovits; Max Herpich; Guang Feng; Alexei A. Kornyshev; Ulrich Stimming

Interface between an Au(111) surface and an ionic liquid: The influence of water on the double layer capacitance

Jochen Friedl, [a] Iulius I. E. Markovits, [b] Max Herpich, [b] Guang Feng, [c] Alexei A. Kornyshev, [d] and Ulrich Stimming*[a,b]

Abstract: The presence of water in **r**oom **t**emperature **i**onic **l**iquids (RTILs) can have a strong effect on their properties. In particular, water adsorption at electrodes can reduce the electrochemical potential window of the system. It is thus important to understand where water will be present depending on the electrode potential, the type of ionic liquid and the electrode material. We investigate the influence of water on RTILs by measuring the potential dependent double layer capacitance of various water-RTIL mixtures. The resulting capacitance versus potential curves are reproduced employing mean-field theory calculations. From the parameters used to obtain the best agreement between experimental and theoretical curves some properties of the RTILs can be deducted, such as a stronger interaction of water with RTIL anions than cations and an agglomeration of water at potentials positive or negative of the potential of zero charge.

Introduction

Solvent-free electrolytes, **r**oom **t**emperature **i**onic **l**iquids (RTILs) have properties in between solid electrolytes and electrolyte solutions with a number of potential applications in electrochemical systems. One of their main advantages is their large potential window, in some cases 4.5-6V [1,2]. The presence of impurities, water in particular, may reduce the width of this potential window [3]. Bulk properties of water-RTIL mixtures were therefore studied extensively [4–7]. Water was found to exist mostly as monomers, often trapped close to hydrophilic moieties [8,9].

The adsorption of water at electrodes has only recently been studied theoretically [10–12] and experimentally [13,14]. Feng et al. studied humid imidazolium-based ionic liquids and the adsorption of water at a carbon-like electrode using molecular dynamics simulations [10]. They found that the adsorption of water increases with potential and that the electrosorption effect is stronger at potentials positive of the potential of zero charge (p.z.c.), due to the stronger interaction of water with the anions.

[a]   Dr. J. Friedl, Prof. U. Stimming
        School of Chemistry
        Newcastle University
        Newcastle upon Tyne, NE1 7RU, United Kingdom
        E-mail: Ulrich.stimming@newcastle.ac.uk
[b]   Dr. I.I.E.Markovits, Mr. M. Herpich, Prof. U Stimming
        TUM CREATE
        1 CREATE Way, #10-02 CREATE Tower, Singapore 138602,
        Singapore
[c]   Prof. G. Feng
        State Key Laboratory of Coal Combustion, School of Energy and
        Power Engineering
        Huazhong University of Science and Technology (HUST)
        Wuhan, 430074, China
[d]   Prof. A.A. Kornyshev
        Department of Chemistry
        Imperial College London
        London, SW7 2AZ, United Kingdom

        Supporting information for this article is given via a link at the end of
        the document.

Motobayahsi and Osawa used Surface Enhanced Infrared Absorption Spectroscopy (SEIRAS) as a tool to detect the presence of water in the electrochemical double layer (ECDL) of a humid imidazolium-based RTIL at an Au electrode [13]. They confirmed that water accumulates at the electrode even at low concentrations and that the adsorption is more pronounced at potentials positive of the p.z.c..
In an atomic force microscopy (AFM) force curve study Zhong et al. found that with increased water content more water molecules adsorb on the Au(111) electrode or interact with the ionic liquid, as evidenced by a decreasing stiffness of the first and second electrolyte layer [14].

Electrochemical impedance spectroscopy (EIS) is a method to determine the double layer capacitance C_{DL} of RTILs [15–21]. Reported shapes of the C_{DL} vs. potential curves show significant deviation and researchers commented on irreproducibility of curves within one study [15,16]. This is believed to be partly due to contaminations (such as water), but might also be caused by reactions taking place within the wide potential window of RTILs [17,20,22]. Therefore, we monitor the water content and limit the potential range of our study to potentials in which only non-faradaic reactions occur (see Fig. 1b).

We investigate an Au(111) electrode in contact with 1-butyl-1-methy-lpyrrolidinium bis[(trifluoromethyl)sulfonyl]imide (PyrTFSI) with various water contents with EIS. Obtained C_{DL} vs. potential curves are compared to those calculated using mean-field theory [23,24] assuming an asymmetric electrosorption of water. The calculated curves share a number of similarities with the experimentally recorded data. Therefore we are able to obtain a more conclusive image of the influence of water on the electrode-RTIL interface:

1. Our results show potential-dependent agglomeration of water in the ECDL, as found by AFM and SEIRAS [13,14];
2. Theoretical predictions regarding the sensitivity of C_{DL} of RTILs towards water are confirmed [10];
3. Theoretical tools such as mean-field theory calculations with the compacity parameter γ of RTILs [23] are shown to be able to reproduce experimental data. From the parameters used in the calculation properties of RTILs, like the preferred interaction of water with anions, can be deducted.

Results and Discussion

Figure 1a shows overview CVs recorded in a potential window from -1.2 V to 1.2 V vs. Pt. They do not show the featureless behavior often associated with RTILs, which has been reported before [17]. The addition of water increases the anodic and cathodic currents that are observed, but also the relatively dry PyrTFSI sample (1.4 water molecules for 1000 RTIL anions or cations) shows a number of redox waves. The anodic peaks at ca. -0.4 V vs. Pt appear only after the reduction at -1.0 V vs. Pt.

CVs recorded immediately before and after EIS in a smaller range are compared in Fig. 1b. The CVs for the dry PyrTFSI (1000 : 1.4, blue) do not deviate much from each other, and the currents seem to be non-faradaic in nature. For the more humid PyrTFSI (1000 : 58.6, red) the deviation of CVs before and after EIS is more pronounced but the current density is low (compare to peak current density of 0.5 mM ferrocene in Fig. S3). One can

assume that the difference in CVs before and after the measurement is due to products formed during the EIS measurements [25].
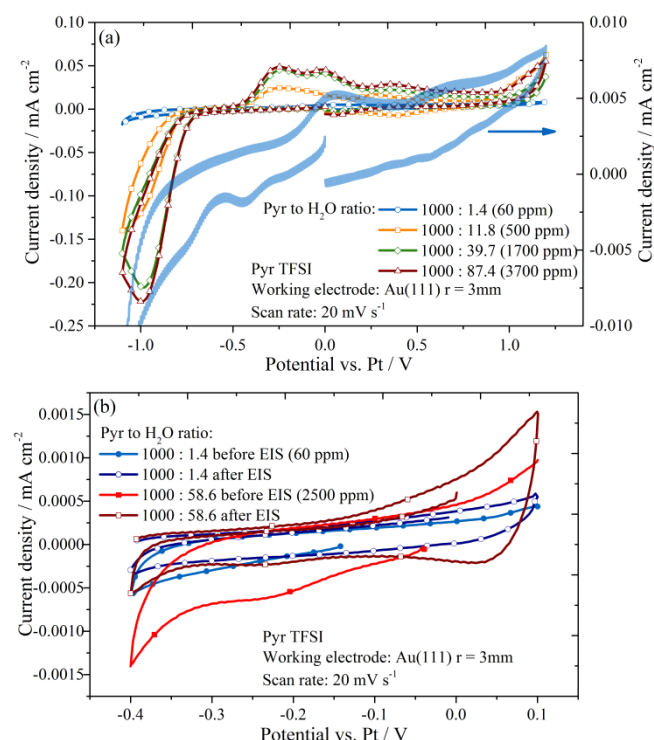

Figure 1. (a) CVs of PyrTFSI with different water contents. The transparent blue curve shows the CV recorded in dry PyrTFSI on a more sensitive scale. (b) CVs of PyrTFSI before and after EIS in the potential region in which EIS was measured.

Using a symmetric electrochemical cell EIS measurements were performed up to 200 kHz. A typical Bode plot Au(111) in humid PyrTFSI (1000:58.6) is shown in Fig. 2a. Multiple fit options for the data and the respective equivalent circuits are shown in the graph:

1. A resistor (R_{Ohm}) and a capacitor (C_{HF}) in series for frequencies $2 \cdot 10^5$ Hz > f >100 Hz. Goodness of fit (details in the SI) for the 51 spectra, $\chi^2 = 0.011$;
2. A resistor (R_{Ohm}) and constant phase element (Q) for all frequencies, $\chi^2 = 0.040$;
3. A resistor (R_{Ohm}) in series to a capacitor (C_{HF}) and a CPE (Q) in parallel for all frequencies [17], $\chi^2 = 0.012$.

A CPE can be converted to a capacitance $C_{surface}$ using the formula for a surface distribution with infinite charge transfer resistance given by Hirschorn et al. [26]. The potential dependence of the double layer capacitances determined with circuits 1 – 3 is shown in Fig. 2b. For circuit 3 the sum of C_{HF} and $C_{surface}$ is shown. The double layer capacitance vs. potential curves are similar for all three curves. Especially at high frequencies the surface roughness should have only a small influence on the ECDL [21]. Two 'peaks' and a general increase with potential can be seen. In the following investigation, C_{HF} from equivalent circuit 1 will be analyzed, the treatment would be
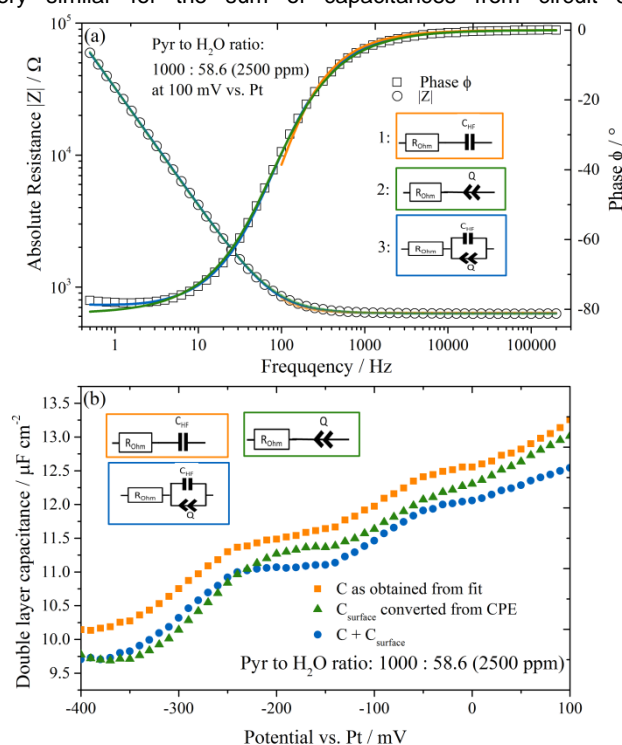
very similar for the sum of capacitances from circuit 3.

Figure 2. (a) Exemplary Bode plots of PyrTFSI (1000 : 58.6) at 100 mV vs. Pt fitted with three equivalent circuits given in the graph. (b) The fitted double layer capacitances over potential curves.

Fig. 3 shows C_{HF} vs. potential curves for five Pyr to H$_2$O ratios. All samples exhibit a peak in the lower half of the potential range and an increasing C_{HF} with increasing potential. For the three samples with highest water content a second peak at higher potentials is present. Subsequent annealing of the electrode led to an increase in surface roughness which explains the variation in magnitude seen in Fig. 3a. The reference electrode shows a certain variation between measurements (see Fig. S3b). Therefore, in order to compare the curves directly, we normalized the C_{HF} of all samples to the first peak value of the driest curve (red, $C_{HF} = 9.42 \ \mu F \ cm^2$) and shifted all curves so that the potential position of the first maximum is at *0 mV*. In 1-butyl-1-methyl-pyrrolidinium bis(trifluoromethylsulfonyl)amide the p.z.c. was found to be in a range from *-0.5 V* to *-0.1 V* vs. Pt at an Au(111) electrode [14]. In 1-butyl-3-methyl-imidazolium hexafluorophosphate the p.z.c. is roughly *-0.4 V* to *-0.2 V* vs. Pt [17,27]. We thus assume that the first peak (at *0 mV* in Fig. 3b) is within ±*100 mV* of the p.z.c.. After the first peak at 0 mV, the red curve remains constant until it increases at an onset potential of roughly 250 mV. With higher water contents the onset shifts to lower potentials and the C_{HF} reaches higher values. For potentials smaller than 0 mV the effects of water are less pronounced.

Since these are the first systematic studies of the influence of small concentrations of water on the ECDL of an RTIL, some factors in this system remain unknown. But, the observed trends can be explained assuming that at positive potentials adsorption of water into the double layer is stronger than at negative potentials. Using simple mean-field theory[23,24] and incorporating an asymmetric electrosorption of water, we can obtain plots of the kind shown in Fig.4. On the negative (left) wing the order of the curves is almost as in the experiment, the curves change less with water content than they do at positive potentials.
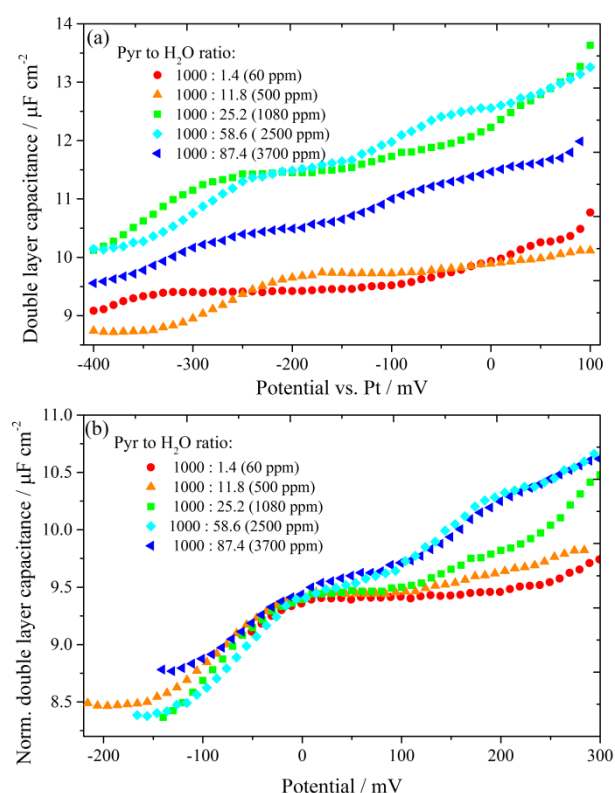
2

Figure 4. Capacitance calculated within the mean field theory of the ECDL and electrosorption of water. Details of parameters used are described in the SI. The red solid curve is for a dry ionic liquid.

Figure 3. (a) C_{HF} over potential curves for different water contents. (b) Shifted and normalized C_{HF} over potential curve.

We describe the equations and parameters used to plot this curves in the SI. The following physical approximations were made:

1. In a certain range of potentials ($-k_BT/e < u < 0.5\,k_BT/e$) around the p.z.c. the water is in depletion.

2. Outside of above range water is electrosorbed, its density becomes more than two times larger than in the bulk. The electrosorption rises steeper with voltage on the positive side of this interval than on the negative side.

3. A homogeneous concentration of water in the ECDL is considered, affecting the effective permittivity that provides dielectric screening of ion-ion interactions and thus increases the C_{DL}. The more water is in the double layer the higher the capacitance. No discrete, layer-to-layer distribution of water is considered in this model.

4. In order to achieve the overall asymmetry of the curve we assume that the maximum possible density of anions is higher than that of cations (in these plots, 4 times higher), and the ability to compress the layer of ions in the potential range positive of p.z.c. is characterized by the compacity parameter $\gamma = 0.4$ (which is a reasonable estimate for the ratio of the average concentration of ions in the bulk of this ionic liquid to the maximum concentration of cations).
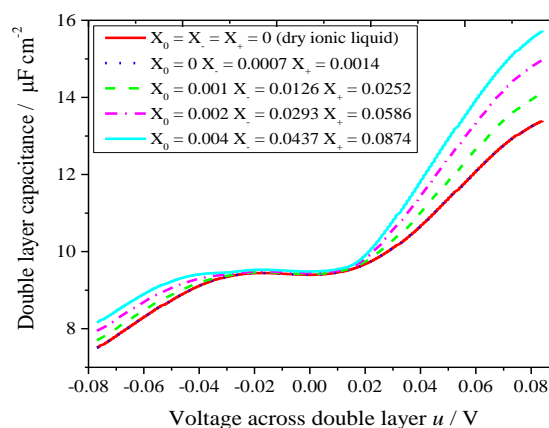
The similarity between the experimental data (Fig. 3b) and theoretical results (Fig. 4) is obvious, however, the following differences appear:

1. The theory gives the second maximum as a top of a bell. So approaching it, the theoretical curves come out concave, whereas the experimental ones are rather convex.

2. The capacitance of the theoretical curves increases with water content. This is also true for the experimental curves in the positive potential region, but in the negative potential branch, the sequence is not maintained. This might be due to the performed normalization. Future experiments with less annealing steps should be able to clarify this discrepancy.

3. The absolute value of capacitance changes in a more pronounced way for the calculated curves than in the experiments; also the potential range in the theoretical curves is smaller. This is a result of a mean-field approximation that does not take into account short range correlations between the ions of the ionic liquid. The inclusion of short range ion-ion correlations will make the interval of capacitance interaction broader, and as a result will suppress the variation of capacitance in the studied potential range. An example of such effect a 'renormalized' plot is shown in Fig. S4.

4. In the theoretical curves, the rise in capacitance with potential at positive potentials is faster than the decline in capacitance at negative potentials. The experimental curves show the opposite trend. Potentially this discrepancy could also be remedied by including short range ion-ion correlations. Further experimental results and a refinement of the theory could clarify this point.

A recent paper by Budkov, Kolesnikov and Kiselev (BKK) [11] extends the model of ref.[23] by including the presence of neutral but polarizable species, such as solvent molecules. They found an elegant method to account for the presence of such a component considering co-solvent molecules at the same footing as ions and within a self-consistent density functional approach a distribution of co-solvent molecules was obtained. This results in a depletion (enrichment) of the co-solvent molecules near the electrode if their polarizability is lower (higher) than that of the RTIL. The enrichment increases with the increase of the voltage drop. However, there is no depletion of the concentration of co-solvent at the electrode relative to the bulk (c.f. Fig.2 of their paper). Like our present simple estimate, as described in the SI, the BKK model does not take into

3

account possible 'freezing' of orientational polarizability of solvent dipoles; their model is better applicable for nonpolar solvent additives. Gongadze and Iglic [12] developed another mean-field model in which the dielectric saturation of solvent molecules with permanent dipole moments has been explicitly considered, but these have not been studied in detail and most importantly the results for capacitance have not been displayed. It might be interesting to combine the two approaches, in an attempt to integrate the dielectric saturation effect into an extended version of the BKK model.

The qualitative trends displayed in BKK's Fig. 4b are similar to those that we observe experimentally and which our simple estimates confirm [11]. This is seen in spite of the fact that the BKK model does not have a depletion of solvent molecules at the electrode as compared to the bulk; what it captures, however, is the increase of the dielectric screening with the electrosorption of polarizable molecules, which is one of the main effects here.

Conclusions

In this study we investigated the potential dependence of the double layer capacitance of an Au(111) electrode immersed in PyrTFSI and systematically varied the water content. Impedance spectra were obtained that could be modeled with two equivalent circuits. C_{DL} vs. potential curves for the various water contents were compared with a prediction made by mean-field theory [23].

Like previous experimental [13,14] and theoretical studies [10–12] our work shows that with increasing absolute potential water adsorbs at the Au(111) surface. In addition, we are able to show that this agglomeration of water has an influence on the C_{DL} [10], *the main signature is the increase in C_{DL} at potentials positive of the p.z.c.*. The higher the water content in the bulk, and correspondingly, in the ECDL, the more the wings of capacitance deviate from the capacitance of the dry ionic liquid case. This was reproduced in computed curves where we assumed a lower compacity value in the anodic range than in the cathodic range. Therefore, the higher affinity of water towards RTIL anions rather than cations as predicted in molecular dynamic simulations [10] was confirmed.

The increased water content leads to dilution of the ionic liquid and therefore to smaller values of the compacity parameter γ [23,24]. This effect alone is very weak, as long as the volume portion of water is small. A stronger effect comes through the influence of an increased concentration of water in the ECDL (electrosorption) on the effective dielectric constant. To qualitatively mimic the experimental curves we assumed a 'silent range' around the p.z.c. where water in the double layer is in depletion.

The future work will be in extending the voltage range of measurement and develop a regular self-consistent theory of water distribution in the double layer and its effect on capacitance along the lines discussed in the previous section and beyond, as well as performing new molecular dynamic simulations. Only then the capacitance measurements may become an additional diagnostic tool of the water sorption in the double layer. This preliminary report, however, paves the way towards this goal.

Experimental Section

High purity grade PyrTFSI was purchased from IoLiTec Ionic Liquids Technologies GmbH and used without further purification. All handling of the RTIL was performed in an Argon-purged glovebox, except for the addition of water which was done outside of the glovebox. As electrode an Au(111) single crystal disk from MaTeck was used (99.999%). The Au(111) crystal was prepared prior to each measurement following the method described by Kibler [28]. The crystal shows terraces of several 100 nm as can be seen in Fig. S1. The water content in PyrTFSI was determined by Karl-Fisher titration with a Metrohm 831 KF Coulometer. The water content is given as ratio between Pyr (or TFSI) ions and H_2O. The notation we use, e.g. 1000 : 58.6, stands for 1000 RTIL cations or anions with average 58.6 water molecules. The Karl-Fisher titration gives a value in ppm which is calculated by the amount of water detected and the mass of the inserted sample. The ppm number given by the Metrohm 831 KF Coulometer is being recalculated to the above ratio by incorporating the mass of the PyrTFSI in the equation. Electrochemistry was performed in a highly symmetric Kel-F cell. Au(111) working electrode and polycrystalline Au counter electrode were placed on the opposite faces of the cell. To achieve low input impedance, a Pt wire was employed as quasi-reference. This reference was reported to be as reliable as Ag wires coated with AgCl or $AgPF_6$ [17]. The stability of the reference electrode was determined by measuring the equilibrium potential of the ferrocene/ferrocenium coupled in PyrTFSI (Fig. S3). We found the Pt wire potential to be stable during measurements but exhibiting a variance of more than 0.2V for successive experiments. Cyclic voltammetry (CV) and EIS were recorded on an SP-300 from Bio-Logic. Once the PyrTFSI was inserted into the cell a CV (20mV/s) was performed from open circuit potential to -0.4 V vs. Pt and reversed to 0.1 V vs. Pt. EIS was performed immediately after the CV, 51 measurements were taken for each sample from 0.1 V to -0.4 V vs. Pt. The potential of the working electrode was adjusted, followed by 2 minutes wait time and EIS from 200 kHz to 0.5 mHz with an amplitude of 10 mV. This was followed by one more CV with the same vertex potentials as before.

EC-STM measurements were performed on a Bruker Multimode 8 with two Pt wires as reference and counter electrodes and the Au(111) crystal as working electrode.

Acknowledgements

[1]   M. C. Buzzeo, C. Hardacre, R. G. Compton, *ChemPhysChem* **2006**, *7*, 176–180.

[2]   N. Bucher, S. U. Hartung, M. Arkhipova, D. Y. W. Yu, P. Kratzer, G. Maas, M. Srinivasan, H. E. Hoster, *RSC Adv.* **2014**, *4*, 1996 – 2003.

[3]   A. M. O'Mahony, D. S. Silvester, L. Aldous, C. Hardacre, R. G. Compton, *J. Chem. Eng. Data* **2008**, *53*, 2884–2891.

[4]   J. L. Anthony, E. J. Maginn, J. F. Brennecke, *J. Phys. Chem. B* **2001**, *105*, 10942–10949.

[5]   S. Rivera-Rubero, S. Baldelli, *J. Am. Chem. Soc.* **2004**, *126*,

4

11788–11789.

[6]   R. Hayes, S. Imberti, G. G. Warr, R. Atkin, *Angew. Chemie - Int. Ed.*
        2012, *51*, 7468–7471.

[7]   L. Cammarata, S. G. Kazarian, P. A. Salter, T. Welton, *Phys. Chem.*
        Chem. Phys. **2001**, *3*, 5192–5200.

[8]   N. Sieffert, G. Wipff, *J. Phys. Chem. B* **2006**, *110*, 13076–13085.

[9]   M. Moreno, F. Castiglione, A. Mele, C. Pasqui, G. Raos, *J. Phys.*
        Chem. B **2008**, *112*, 7826–7836.

[10]   G. Feng, X. Jiang, R. Qiao, A. A. Kornyshev, *ACS Nano* **2014**, *8*,
        11685–11694.

[11]   Y. A. Budkov, A. L. Kolesnikov, M. G. Kiselev, *J. Chem. Phys.* **2016**,
        144, 184703.

[12]   E. Gongadze, A. Iglič, *Electrochim. Acta* **2015**, *178*, 541–545.

[13]   K. Motobayashi, M. Osawa, *Electrochem. commun.* **2016**, *65*, 14–17.

[14]   Y. Zhong, J. Yan, M. Li, L. Chen, B. Mao, *ChemElectroChem* **2016**,
        1–7.

[15]   V. Lockett, M. Horne, R. Sedev, T. Rodopoulos, J. Ralston, *Phys.*
        Chem. Chem. Phys. **2010**, *12*, 12499–512.

[16]   T. Pajkossy, D. M. Kolb, *Electrochem. commun.* **2011**, *13*, 284–286.

[17]   M. Gnahm, T. Pajkossy, D. M. Kolb, *Electrochim. Acta* **2010**, *55*,
        6212–6217.

[18]   M. T. Alam, M. Mominul Islam, T. Okajima, T. Ohsaka, *Electrochem.*

[19]   F. Silva, C. Gomes, M. Figueiredo, R. Costa, A. Martins, C. M.
        Pereira, *J. Electroanal. Chem.* **2008**, *622*, 153–160.

[20]   R. Atkin, N. Borisenko, M. Drüschler, F. Endres, R. Hayes, B. Huber,
        B. Roling, *J. Mol. Liq.* **2014**, *192*, 44–54.

[21]   T. Jänsch, J. Wallauer, B. Roling, *J. Phys. Chem. C* **2015**, *119*,
        4620–4626.

[22]   D. S. Silvester, R. G. Compton, *Z. Phys. Chem* **2006**, *220*, 1247–
        1274.

[23]   A. A. Kornyshev, *J. Phys. Chem. B* **2007**, *111*, 5545–57.

[24]   A. A. Kornyshev, *J. Phys. Chem. B* **2007**, *111*, 5545–5557.

[25]   R. P. Swatloski, J. D. Holbrey, R. D. Rogers, *Green Chem.* **2003**, *5*,
        361.

[26]   B. Hirschorn, M. E. Orazem, B. Tribollet, V. Vivier, I. Frateur, M.
        Musiani, *Electrochim. Acta* **2010**, *55*, 6218–6227.

[27]   S. Eisele, M. Schwarz, B. Speiser, C. Tittel, *Electrochim. Acta* **2006**,
        51, 5304–5306.

[28]   L. A Kibler, *Int. Soc. Electrochem.* **2003**, 1–56.

commun. **2007**, *9*, 2370–2374.

Accepted Manuscript

ARTICLE

Entry for the Table of Contents

ARTICLE

The interface between an Au(111) electrode and an ionic liquid with varying water contents was investigated by electrochemical impedance spectroscopy. Obtained double layer capacitance versus potential curves show that water adsorbs at the electrode and increases the capacitance. These curves were reproduced with mean field theory calculations.
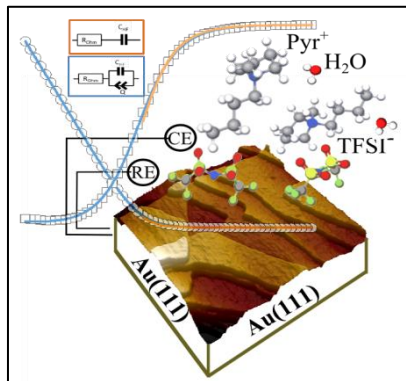
Jochen Friedl, Iulius I. E. Markovits, Max Herpich, Guang Feng, Alexei A. Kornyshev, and Ulrich Stimming

Page No. – Page No.

Interface between an Au(111) surface and an ionic liquid: The influence of water on the double layer capacitance